Molecular Transport of *n*-Alkanes Through Diol Chain-Extended Polyurethane Membranes

B. K. Kendaganna Swamy,[1] Siddaramaiah,[2] B. Vijaya Kumar Naidu,[3] N. N. Mallikarjuna,[3] T. M. Aminabahvi[3]

[1]Department of Chemistry, J.S.S. College, Mysore, 570 004, India
[2]Department of Polymer Science and Technology, S.J. College of Engineering, Mysore, 570 006, India
[3]Membrane Separations Division, Center of Excellence in Polymer Science; Karnatak University, Dharwad, 580 003, India

ABSTRACT: Molecular transport of *n*-alkanes was investigated by calculating sorption, diffusion, and permeation of liquids through the diol chain-extended polyurethane (PU) membranes in the temperature interval 25–60°C. Sorption experiments were performed gravimetrically. Diffusion coefficients were calculated from Fick's equation. These results showed a dependency on the nature and size of interacting *n*-alkane molecules as well as morphology of the chain-extended PUs. Transport kinetics followed an anomalous trend. Using the temperature-dependent transport parameters, activation energies were calculated for diffusion and permeation processes using an Arrhenius equation. The van't Hoff relationship was used to obtain enthalpy and entropy of sorption. Concentration profiles of liquids through PU membranes were computed using Fick's equation, solved under appropriate initial and boundary conditions. A correlation was attempted between transport properties of liquids and physicomechanical properties of PU membranes. © 2005 Wiley Periodicals, Inc. J Appl Polym Sci 96: 874–882, 2005

Key words: polyurethanes; membranes; diffusion; physicomechanical properties; transport kinetics

INTRODUCTION

Polyurethane (PU) elastomers are the well-known engineering flexible polymers that exhibit unique mechanical properties, primarily as a result of two-phase morphology. These polymers have alternating block copolymers made of hard segments of aromatic groups from the diisocyanate/chain extender and soft segments of aliphatic chains from the diol (ether or ester).[1–3] Hard and soft segments are chemically incompatible and microphase separation of hard segments into domains dispersed in a matrix of soft segments can occur to varying degrees. Chain-extended PUs find a wide variety of engineering applications because of their diversified engineering properties useful as coatings, adhesives, and biomedical applications, for example, these PUs are well known for their good mechanical properties.[4,5] In commercial applications of PU, it is likely that they come into contact with organic liquids and, thus, interactions of PU chains with organic molecules are of relevance before their successful industrial applications. In view of this, molecular transport studies on PU membranes with organic liquids have been extensively investigated over the past decade.[6–8] In these studies, we observed that sorption, diffusion, and permeation of *n*-alkanes (C_6–C_9) through segmented PU membranes were influenced by the physical and chemical nature, morphology, and crosslink density of the polymer in addition to temperature, shape, and size of the interacting molecules.[9,10]

With the ever-increasing importance of polymer blends in engineering areas,[11,12] studies have been directed to develop chain-extended PUs.[13] Swelling of such polymers can be used to understand the polymer–solvent interactions. A search of the literature revealed no systematic studies on sorption, diffusion, and swelling of natural polyol (caster oil) based diol chain-extended PUs with *n*-alkanes, although a few studies have been published with respect to commercial PU membranes.[14,15] In view of the importance of PU as a membrane in engineering applications and in continuation of our ongoing program of research on molecular transport,[6–10] we present here transport data on butane 1,4-diol (BD) and hexane 1,6-diol (HD) based chain-extended PUs with *n*-hexane, *n*-heptane,

n-octane, and *n*-nonane. Diffusion coefficients were computed from Fick's diffusion equation. Permeability coefficients were calculated from sorption and diffusion results. Sorption results were used to compute concentration profiles at different depths along the membrane thickness and at different time intervals by solving Fick's equation, using appropriate initial and boundary conditions, based on the numerical simulation scheme using a finite-difference approach.[16–19]

EXPERIMENTAL

Materials

Castor oil [CO; number-average molecular weight (M_n) = 930; hydroxyl number = 160 to 168; acid value = 2.45; isocyanate equivalent = 30] was obtained from the local market. Toluene-2–4-diisocyanate (TDI), 4,4'-methylenebis (phenylisocyanate) (MDI), hexamethylene diisocyanate (HMDI), and dibutyl tin dilaurate (DBTL) were obtained from Sigma–Aldrich (Milwaukee, WI) and were used as received. Chain extenders, 1,4-butane diol and 1,6-hexane diol, were obtained from Fluka Chemie (Buchs, Switzerland). Toluene, *n*-hexane, *n*-heptane, *n*-octane, *n*-nonane, and methyl ethyl ketone (MEK) were all of AR grade samples and distilled before use.

Synthesis of chain-extended polyurethane membranes

Castor oil (0.001 mol) was dissolved in 50 mL of MEK and reacted with diisocyanate (0.0022 mol) using 2–3 drops of DBTL as a catalyst in a 250-mL three-neck round-bottom flask. The contents were stirred on a magnetic stirrer for 1 h at 70°C. The prepolyurethane formed was reacted with an equal molar ratio (0.001 mol) of diol dissolved in MEK. The mixture was stirred for another 15–20 min at 70°C to form a uniform mixture and poured onto a clean glass plate kept in a preheated circulating air oven at 70°C for 24 h. The membrane thus formed was cooled and removed from the mold. A similar procedure was adopted for all other preparations. The golden yellow colored transparent and toughened diol chain-extended PU films were obtained.

The chemical structure of the chain-extended PU is given in Scheme 1. Six types of PUs with different diisocyanates and diols were prepared following the above procedure and were designated as

- CO + TDI + 1,4-diol (PU-1)
- CO + TDI + 1,6-diol (PU-2)
- CO + MDI + 1,4-diol (PU-3)
- CO + MDI + 1,6-diol (PU-4)
- CO + HMDI + 1,4-diol (PU-5)
- CO + HMDI + 1,6-diol (PU-6)
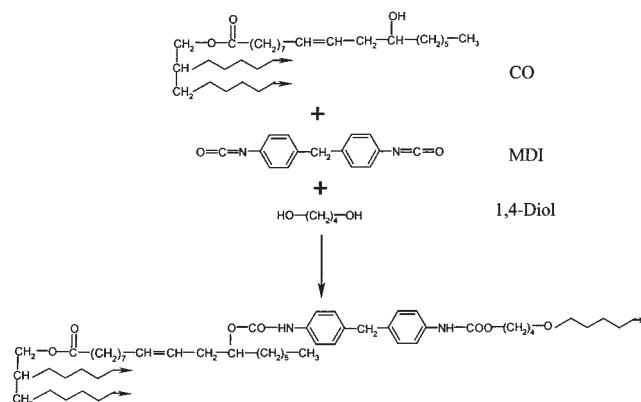
Scheme 1

Specimen preparation

The prepared PU samples were cut circularly (diameter = 1.76 cm) using a sharp-edged steel die. The thickness of the specimen varied from 0.20 to 0.26 cm. Samples were dried in a desiccator before use. Dry weights of the cut samples were taken before immersion into airtight, metal-capped test bottles containing *n*-alkanes for subsequent sorption experiments.

Physicomechanical properties

The diol-based chain-extended PUs were characterized for density and surface hardness (Shore A and Shore B) according to ASTM D 792-86 and ASTM D 785 methods, respectively. Tensile strength, % elongation at break, and tensile modulus were measured according to ASTM D 368 using a 4302 model Hounsfield universal testing machine (Redhill, UK). At least five samples were chosen for testing at room temperature for each formulation and average values are reported in Table I.

Sorption experiments

Sorption experiments were performed at 25, 40, and 60°C by immersing the cut membrane samples in test media (*n*-alkanes) taken in screw-tight metal-capped bottles maintained at the desired constant temperature (±0.5°C) in a thermostatically controlled oven. At specified intervals of time, membranes were removed from the containers, surfaces were dried between smooth filter paper wraps, and weighed immediately using an analytical balance to an accuracy of ±0.01 mg. The specimens were then placed immediately into the test liquid and transferred to the temperature-controlled oven. Total time spent by the membrane outside the solvent was kept at a minimum (say, ∼ 30–50 s) to minimize the experimental error arising from evaporation losses. Weighing of samples was continued until attainment of equilibrium sorption.

TABLE I
Physicomechanical Properties of Diol Chain-Extended Polyurethanes

PU sample	Sample code	Tensile strength (MPa) ($\pm 2\%$)	% Elongation at break $\pm$ ($\pm 3\%$)	Tensile modulus (MPa) ($\pm 2\%$)	Surface hardness		Density (g/cm^3)
					Shore A	Shore D	
CO + TDI + 1,4-diol	PU-1	1.25	156	6.7	70	46	1.058
CO + TDI + 1,6-diol	PU-2	1.05	136	4.8	69	50	1.127
CO + MDI + 1,4-diol	PU-3	1.29	162	5.0	76	48	1.041
CO + MDI + 1,6-diol	PU-4	1.10	137	4.2	78	59	1.105
CO + HMDI + 1,4-diol	PU-5	1.18	147	3.8	55	38	1.028
CO + HMDI + 1,6-diol	PU-6	0.99	124	2.8	65	36	1.086

The time taken to reach equilibrium sorption for different liquids varied from 70 to 90 h, depending on the nature of the n-alkanes. The % weight gain Q_t of the sorbed membrane was calculated as

$$Q_t = \left(\frac{M_t - M_i}{M_i} \right) \times 100 \qquad (1)$$

where M_i is the initial dry weight of the membrane and M_t is the weight of the sorbed membrane at time, t.

RESULTS AND DISCUSSION

Physicomechanical properties

Physicomechanical properties of all PUs are presented in Table I. Densities varied between 1.028 and 1.127 g/cm^3, depending on the nature of the chain extender used. For 1,4-diol–based PUs, densities were lower than those observed for 1,6-diol–based PUs. This could be attributable to higher crosslink density as a result of long chain-extended 1,6-diol rather than 1,4-diol. Surface hardness values reflect the resistance to local deformation, which could be related to degree of crystallinity, crosslink density, and porosity of the polymer. Shore A hardness values ranged between 55 and 78, whereas Shore B varied from 36 to 59. Surface hardness values for 1,6-diol–based PUs were generally higher than those observed for 1,4-diol extended PUs, suggesting higher dimensional stability of 1,6-diol extended PUs than that of 1,4-diol extended PUs.

Tensile strength values were found to depend on the type of chain extender used. These values were higher for 1,4-diol–based chain-extended PUs than those for 1,6-diol–based extended PUs. Tensile strength with respect to diisocyanates varied according to the sequence: MDI > TDI > HMDI. The % elongation at break ranged between 124 and 162; these results were higher for 1,4-diol chain-extended PUs than those for 1,6-diol extended PUs. Tensile moduli varied between 2.8 and 6.7 MPa. The lowest tensile modulus of 2.8 MPa was observed for 1,6-diol extended HMDI-based PU, whereas the highest value was observed for 1,4-diol–based TDI containing PU. This indicates the poor dimensional stability of HMDI-based systems than that of the aromatic diisocyanate–based PUs. In all cases, 1,4 diol chain-extended PUs showed higher tensile modulus than that of 1,6-diol–based PUs, indicating that 1,4-diol–based PUs have mechanical properties that are superior to those of the 1,6-diol chain-extended PUs.

Sorption equilibrium

Sorption curves of n-alkanes expressed as mass % uptake (Q_t) versus square root of time at 25, 40, and 60°C are displayed in Figure 1 for PU-1. Sorption occurs as a result of rapid solvent diffusion in relation to polymeric chain relaxation.[10,20] Irregular trends in sorption curves could be attributable to deviations in the rates of molecular chain relaxation arising from locally induced stresses in the polymer matrix. In the present systems, regularly increasing mass uptake trends were observed as a result of ingression of a large number of solvent molecules inside the free-volume voids of the polymer chains. However, the time required in attaining equilibrium sorption varied depending on polymer morphology in addition to the nature of penetrant molecule. An examination of sorption curves (Fig. 1) suggests a systematic trend with respect to molecular volume of n-alkanes. Even though sorption attained equilibrium within 25 min from the beginning of sorption experiment for all n-alkanes, experiments were nevertheless continued for a longer time to ensure complete attainment of equilibrium sorption.

In this study, effects of the nature of diisocyanates on sorption behavior of PU membranes were investigated. Typical sorption curves for 1,4-diol chain-extended PU membranes with different diisocyanates are shown in Figure 2 for n-octane at 40°C. Here, a higher mass uptake was observed for HMDI-based PU membranes than that of TDI- and MDI-based PU membranes. The reason for this is that MDI- and TDI-based PUs possess a greater number of hard segments,
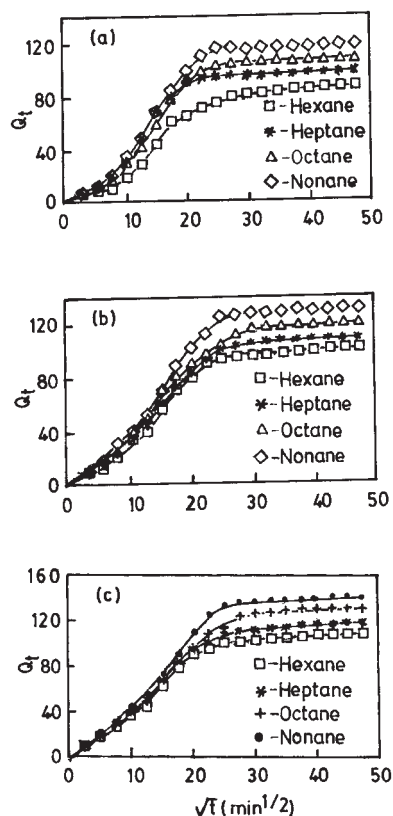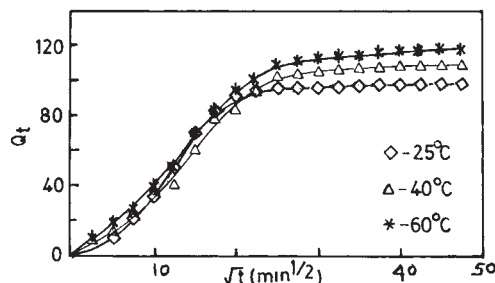
Figure 1 Plot of percentage mass uptake Q_t of PU-1 versus $t^{1/2}$ with different n-alkanes at (a) 25°C, (b) 40°C, and (c) 60°C.

thus creating a tortuous[21] path, giving a slow diffusion of n-alkanes, and thus the equilibrium uptake value was smaller. However, with decreasing number of hard segments, the size of the crystalline phase also decreased, although the number of soft segment increased. Thus, the contact between soft domains increased, thereby leading to a higher penetrant uptake. Because soft domains form a continuous phase, diffusion may therefore be continuous in the soft phase (amorphous). Thus, a sharp increase in uptake was observed.
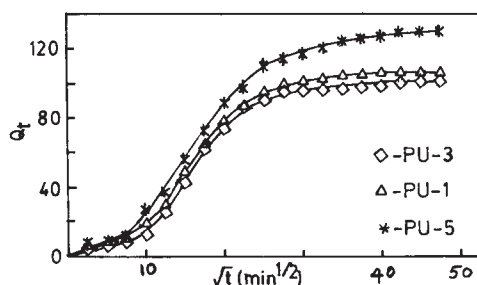
Figure 2 Plot of percentage mass uptake Q_t versus $t^{1/2}$ for chain-extended PUs with different diisocyanates in n-octane at 40°C.

Figure 3 Plot of percentage mass uptake Q_t versus $t^{1/2}$ for PU-1 in n-octane.

Molecular transport of liquids through polymeric membranes depends on temperature, and thus we studied the effect of temperature on sorption. Such dependency is typically shown in Figure 3 for n-octane for 1,4-diol chain-extended PU. Shapes of sorption curves at 25°C are similar to those at 40 and 60°C, even though the initial slopes of the curves are more pronounced between 25 and 40°C than between 40 and 60°C. Equilibrium sorption increased with increasing temperature because of the increase in free volume at higher temperature.[22]

Values of sorption coefficient S, given in Table II, were obtained from the plateau regions of the equilibrium sorption curves. In all cases, sorption increased with increasing size of n-alkanes (i.e., C_6 to C_9). However, a higher value of S of 1.86 g/g for PU-6 at 60°C with n-nonane could be the result of its compact segment structure in the presence of HMDI and HD. Lower S value of 0.80 g/g for PU-3 at 25°C in n-hexane could be attributable to the presence of hard segments (phenyl) or to molecular symmetry in methylene diisocyanate–based PU membranes. HMDI diisocyanate–based PUs showed higher S values than those of TDI- and MDI-based PUs. Also, sorption values were higher for 1,6-diol–based PUs than those for 1,4-diol–based PUs. Variation of S among different diisocyanates exhibited opposite trends to those of tensile strengths of the same PUs. As the tensile strength increased, the value of S decreased because hard segments of PUs might have induced lower swelling of PUs.

Sorption kinetics

To investigate the nature of diffusion kinetics we analyzed the sorption data, using the following equation[23–25] to compute n and K:

$$\log\left(\frac{M_t}{M_\infty}\right) = \log K + n \log t \qquad (2)$$

where K and n are empirical parameters; and M_t and M_∞ are mass uptake values at time t and at equilib-

TABLE II
Diffusion D, Sorption S, Permeation P, Coefficients and Thermodynamic Sorption Constant (K_s) of Different Diol Chain-Extended PUs in n-Alkanes at Different Temperatures

PU sample	T (°C)	Hexane				Heptane				Octane				Nonane			
		$D \times 10^7$ (cm²/s)	$S \times 10^2$ (g/g)	$K_s \times 10^2$	$P \times 10^7$ (cm²/s)	$D \times 10^7$ (cm²/s)	$S \times 10^2$ (g/g)	$K_s \times 10^2$	$P \times 10^7$ (cm²/s)	$D \times 10^7$ (cm²/s)	$S \times 10^2$ (g/g)	$K_s \times 10^2$	$P \times 10^7$ (cm²/s)	$D \times 10^7$ (cm²/s)	$S \times 10^2$ (g/g)	$K_s \times 10^2$	$P \times 10^7$ (cm²/s)
PU-1	25	2.65	86	1.00	2.40	1.23	98	0.98	1.20	0.86	107	0.93	0.92	0.68	118	0.92	0.80
	40	4.00	100	1.16	4.00	1.42	108	1.08	1.53	1.32	119	1.04	1.57	0.92	130	1.01	1.19
	60	4.30	108	1.25	4.64	1.72	118	1.18	1.02	1.62	128	1.12	2.07	1.34	140	1.09	1.87
PU-2	25	3.29	98	1.13	3.22	1.32	110	1.10	1.22	1.22	120	1.05	1.46	0.92	132	1.03	1.21
	40	4.39	112	1.30	4.91	1.62	121	1.21	1.96	1.60	132	1.15	2.11	0.98	148	1.15	1.45
	60	4.78	126	1.46	6.02	1.83	137	1.37	3.11	1.72	148	1.29	2.54	1.35	160	1.25	2.16
PU-3	25	1.79	80	0.93	2.16	1.20	92	0.92	1.10	0.84	102	0.89	0.85	0.63	112	0.87	0.70
	40	2.98	107	1.24	3.18	1.39	100	1.00	1.39	1.29	112	0.98	1.44	0.89	126	0.98	1.12
	60	3.58	119	1.38	4.26	1.68	108	1.08	1.81	1.58	120	1.05	1.89	1.27	132	1.03	1.67
PU-4	25	2.31	92	1.06	2.12	1.28	98	0.98	1.25	1.19	117	1.02	1.39	0.88	124	0.96	1.09
	40	3.24	109	1.26	3.53	1.52	116	1.16	1.76	1.51	126	1.10	1.90	0.92	136	1.06	1.25
	60	3.78	121	1.40	4.57	1.75	128	1.28	2.24	1.64	134	1.17	2.19	1.29	151	1.17	1.94
PU-5	25	4.32	110	1.27	4.75	4.2	118	1.18	4.95	3.89	130	1.14	5.05	3.72	141	1.10	5.24
	40	4.82	119	1.38	5.73	4.45	126	1.26	5.00	4.02	141	1.25	5.66	3.86	152	1.18	5.86
	60	5.02	128	1.48	6.42	4.86	140	1.40	6.80	4.16	152	1.33	6.32	3.95	168	1.31	6.63
PU-6	25	4.58	130	1.51	5.95	4.32	142	1.42	6.13	4.25	158	1.38	6.71	4.06	161	1.25	6.53
	40	5.06	140	1.62	7.08	4.83	150	1.50	7.24	4.62	162	1.42	7.48	4.36	175	1.36	7.63
	60	5.23	154	1.79	8.05	4.96	162	1.62	8.03	4.76	173	1.51	8.23	4.56	186	1.45	8.48

rium time t_∞, respectively. The magnitude of n decides the nature of transport kinetics. For instance, $n = 0.5$ for Fickian transport. If $n = 1$, transport follows a non-Fickian trend. In the present study, intermediate values of n, ranging between 0.5 and 1, were indicative of an anomalous type diffusion kinetics.[6–10] To determine n and K, plots of $\log(M_t/M_\infty)$ versus $\log t$ were constructed. The average uncertainty in the estimations of n and K were around ± 0.01 and ± 0.008, respectively. Values of n did not show any systematic variation with temperature (see Table III). However, a general variation of n, from a minimum of 0.55 to a maximum of 0.61, indicated the anomalous type transport phenomenon. Diffusion deviated slightly from a Fickian trend, but not to a greater extent. This fact was substantiated from the observed slight curvature of Q_t versus $t^{1/2}$ curves shown in Figures 1–3. Such observations were also evident from the work of Nicolais et al.,[26] for n-hexane transport in glassy polystyrene.

Diffusion and permeation coefficients

From the slope, θ of the initial linear portion of sorption curves (i.e., Q_t versus $t^{1/2}$) diffusion coefficient was calculated using Fick's equation[21]

$$D = \pi \left[\frac{h\theta}{4M_\infty} \right]^2 \qquad (3)$$

Here, h is thickness of the membrane and M_∞ is the mass uptake at equilibrium time. Triplicate measure-

TABLE III
Analysis of Sorption Data According to Eq. (2) for Diol Chain-Extended PU Systems in n-Alkanes at Different Temperatures

n-Alkane	T (°C)	$n \pm 0.001$						$K \times 10^2$ (g g^{-1} h^{-1})					
		PU-1	PU-2	PU-3	PU-4	PU-5	PU-6	PU-1	PU-2	PU-3	PU-4	PU-5	PU-6
Hexane	25	0.554	0.568	0.562	0.572	0.583	0.590	1.47	1.38	1.32	1.52	1.85	2.26
	40	0.589	0.573	0.592	0.601	0.592	0.598	2.52	2.48	2.38	2.40	2.39	2.95
	60	0.598	0.582	0.608	0.609	0.600	0.608	3.14	4.09	3.02	3.26	3.62	4.02
Heptane	25	0.567	0.572	0.578	0.582	0.583	0.592	1.48	1.59	1.82	1.95	1.95	2.00
	40	0.600	0.612	0.602	0.603	0.608	0.612	2.86	2.98	2.72	3.06	2.69	3.82
	60	0.598	0.603	0.600	0.610	0.610	0.611	4.26	4.28	4.10	4.65	3.82	4.00
Octane	25	0.561	0.570	0.579	0.590	0.583	0.592	1.98	1.86	1.76	2.00	1.95	1.86
	40	0.556	0.563	0.571	0.586	0.582	0.590	3.08	2.86	3.02	3.42	3.28	2.62
	60	0.594	0.602	0.602	0.608	0.608	0.610	4.86	4.52	4.32	4.52	3.68	4.68
Nonane	25	0.566	0.571	0.578	0.586	0.588	0.590	1.62	1.38	1.52	1.62	1.72	1.70
	40	0.585	0.593	0.590	0.598	0.610	0.612	4.38	3.52	3.42	3.18	3.92	2.92
	60	0.581	0.596	0.598	0.610	0.602	0.608	5.62	4.38	5.21	4.29	4.26	4.62

ment of D from sorption curves gave D values within an error of ±0.003 at 25°C, ±0.004 at 40°C, and ±0.005 at 60°C for all PU + *n*-alkane systems (see Table II). Diffusion coefficients decreased with increasing molecular volume of the migrating liquids from *n*-hexane to *n*-nonane. Such an inverse dependency of D on molecular volume of *n*-alkanes suggested that larger molecules in a related homologous series occupy larger free volumes, leading to hindered diffusion through the polymer matrix.[27]

The permeability coefficient P, calculated[28] using $P = DS$, also followed the same trends as that of D. HMDI diisocyanate–based PUs showed higher S and D values than those of TDI- and MDI-based PUs. Sorption and diffusion values were higher for 1,6-diol–based PUs than those for 1,4-diol–based PUs. Variations of S and D within different diisocyantes exhibited the opposite trends to those of tensile strength values of the same PUs. As the tensile strength increased, sorption coefficients decreased because hard segments of PUs might have caused lesser swelling of PUs.

Thermodynamic parameters and activation parameters

Using sorption data, we calculated the equilibrium sorption constant K_S, by considering equilibrium sorption at constant temperature and pressure, using the following equation:

K_S = number of moles of penetrant sorbed/

unit mass of the polymer   (4)

These data are also included in Table II. A systematic decrease in K_S with increasing molecular volume of *n*-alkane was observed, suggesting an inverse dependency of K_S on molecular volume of *n*-alkanes. This could be logical because larger size molecules occupy more free volume than smaller molecules in the amorphous regions of PU, according to free volume theory propositions.[29–31] It has been well documented that free volume of a rubbery or glassy polymer is related to transport parameters of small liquid molecules.[30,31]

Temperature-dependent values of K_S were fitted to the van't Hoff equation[23] to estimate enthalpy (i.e., heat of sorption) ΔH^0 and standard entropy ΔS^0 of sorption, as follows:

$$\log K_S = \left(\frac{\Delta S^0}{2.303R}\right) - \left(\frac{\Delta H^0}{2.303R}\right) \times \left(\frac{1}{T}\right) \quad (5)$$

Estimated values of ΔH^0 and ΔS^0 are given in Table IV. The average estimated error in ΔH^0 was about ± 4 J/mol, whereas for ΔS^0 it was about ±1 J mol^{-1} K^{-1}. The ΔH^0 values were low for PU-6 membrane, sug-

TABLE IV
Activation Energy for Permeation (E_P, kJ/mol), Activation Energy for Diffusion (E_D, kJ/mol), Enthalpy of Sorption (ΔH_s kJ/mol $\pm$ 4) and Entropy of Sorption (ΔS^0, J mol^{-1} K^{-1} $\pm$ 1) for Chain-Extended PU–*n*-Alkane Systems

PU sample	Activation parameter	Hexane	Heptane	Octane	Nonane
PU-1	E_P	9.65	10.36	11.26	12.65
	E_D	5.86	7.49	8.38	9.54
	ΔH_S	45.72	66.51	62.30	58.01
	$-\Delta S$	35.33	35.86	38.82	37.24
PU-2	E_P	10.20	11.30	10.95	11.24
	E_D	6.82	9.02	7.82	8.32
	ΔH_s	66.51	62.38	78.98	91.45
	$-\Delta S$	32.00	34.25	37.32	35.83
PU-3	E_P	14.30	17.86	20.26	23.23
	E_D	11.42	15.36	18.12	20.22
	ΔH_S	54.04	70.16	54.04	74.82
	$-\Delta S$	32.84	34.83	37.99	36.41
PU-4	E_P	15.83	21.62	20.32	25.12
	E_D	12.01	18.38	20.36	24.36
	ΔH_S	58.19	91.45	45.72	66.51
	$-\Delta S$	27.02	33.92	36.78	35.33
PU-5	E_P	12.00	16.36	15.23	18.32
	E_D	9.83	13.00	12.62	15.26
	ΔH_S	41.57	49.95	49.90	58.01
	$-\Delta S$	26.77	34.08	37.41	35.95
PU-6	E_P	14.21	13.62	16.32	15.22
	E_D	8.02	7.42	10.36	12.89
	ΔH_S	49.90	54.04	48.80	49.90
	$-\Delta S$	26.39	32.08	35.58	34.83

gesting its stronger specific interactions with *n*-alkanes. Comparatively higher values of ΔH^0 for PU-2 confirmed higher interactions arising from endothermic sorption. For all PU-*n*-alkane systems, values of ΔH^0 were positive, suggesting endothermic sorption dominated by Henry's mode (i.e., sorption could proceed as a result of creation of new pores in the membrane matrix).[27] From Figure 3, it can be seen that plots vary systematically with temperature in the interval of 25 to 60°C. The calculated ΔS^0 values are negative for all PU-*n*-alkane systems, suggesting that solvent molecules retained their liquid-state structure even in the sorbed state.

Arrhenius activation energies for diffusion (E_D) and permeation (E_P) were computed from: $X = X_0\exp(-E_x/RT)$, where $X = D$ or P, $X_0 = D_0$ or P_0, E_x represents E_D for diffusion and E_P for permeation, and R is the molar gas constant. These data are also included in Table IV. Values of E_D and E_P varied from 5.86 to 24.36 and 9.65 to 25.12 kJ/mol, respectively. These were within the range expected for rubbery polymers, well above their glass-transition temperatures. The E_D values increased systematically with increasing molecular volume of *n*-alkanes, following Eyring's hole theory.[22,27] The larger permeating molecules in a related homologous series of *n*-alkanes (i.e.,

C_6 to C_9) will have larger E_D values and smaller D. Values of E_P were higher than E_D for all PU–n-alkane systems because of the higher degree of cohesive energy of the polymer. Higher values of ΔS^0 for PU-1 and lower values of ΔS^0 were observed for PU-5. Liquids with lower values of D have shown higher E_D and vice versa, although there is no systematic variation of E_P with molecular volumes of n-alkanes.

Computation of concentration profiles

For successful applications of PU membranes in engineering areas, it is important to know the extent of liquid ingression as a function of time and depth of penetration. We have computed liquid concentration profiles for n-alkanes migrating through the PU membrane by solving Fick's second-order differential equation [i.e., eq. (6)] under appropriate initial and boundary conditions. This yielded eq. (7) for solvent uptake $C_{(x,t)}$ of the membrane of thickness h, as a function of time t and distance x along the membrane thickness direction,[16–18] as follows:

$$\frac{\partial C}{\partial t} = D\left(\frac{\partial^2 C}{\partial x^2}\right) \tag{6}$$

$$\left[\frac{C[x, t)]}{C_\infty}\right] = 1 - \frac{4}{\pi} \sum_{m=0}^{\infty} \frac{1}{(2m - 1)} \exp$$

$$\left[-\frac{D(2m - 1)^2 \pi^2 t}{h^2}\right] \sin\left[\frac{(2m - 1)\pi x}{h}\right] \tag{7}$$

In eq. (7), m is an integer and D is the diffusion coefficient computed from eq. (3). To derive eq. (7) from eq. (6), several assumptions were made[16–18]: (1) when the membrane is soaked in a liquid, its concentration on both surfaces immediately reaches equilibrium, (2) the time required to attain thermal equilibrium for the membrane is negligible compared to sorption (immersion) time, and (3) changes in dimensions of the membrane are negligible (i.e., negligible swelling) during liquid immersion experiments. Then, by using the following boundary conditions

$$\begin{array}{llll} t = 0 & 0 < x < h & C = 0 \\ t > 0 & x = 0 & x = h & C = C_x \end{array} \tag{8}$$

we generated concentration profiles at different exposure times for imaginarily varying depths of liquid penetration into membranes. These were computed writing programs in C language and using the procedure developed previously.[18]

Numerical solutions of eq. (7) were obtained from a finite-difference method. Partial differential equations were converted into algebraic equations (more accurately, difference equations). Instead of using the con-

tinuous variable x, we selected a discrete set of points $\{x_j\}$ and instead of time t we selected the set $\{t_i\}$. Likewise, the concentrations would be $C_{i,j}$ and derivatives are given as

$$\frac{\partial C}{\partial t} \simeq \frac{C_{i+1,j} - C_{i,j}}{\Delta t} \tag{9}$$

and

$$\frac{\partial^2 C}{\partial x^2} \simeq \frac{C_{i,j+1} - 2C_{i,j} + C_{i,j-1}}{(\Delta x)^2} \tag{10}$$

In eqs. (9) and (10), higher-order terms were eliminated during computations. Upon inserting eqs. (9) and (10) into eq. (6) and rearranging, we obtain

$$C_{i+1,j} = C_{i,j} + \frac{D(\Delta t)}{(\Delta x)^2} + (C_{i,j+1} - 2C_{i,j} + C_{i,j+1}) \tag{11}$$

where increments $\Delta t = t_{i+1} - t_i$ and $\Delta x = x_{j+1} - x_j$ are constants. If the initial concentration profiles C_{ij} are known, then eq. (11) provides a means of moving up in time to C_{i+1} (upward curve). Such iterations were continued until numerical approximation to equilibrium or steady state was achieved (minima). Values of Δt were then used in the numerical analysis and the membrane was divided into a number of finite slices of equal thickness (Δx) by the concentration-difference planes.

Concentration profiles generated for the PU-1 membrane at 25°C for n-alkanes are shown in Figure 4, wherein it was observed that values of $C_{(x,t)}/C_\infty$ decreased with increasing size of n-alkanes. Concentration profiles changed smoothly within the membrane matrix at different thicknesses. When D increased with concentration, then a sharp solvent front was observed because for the same concentration gradient, the flux increased, resulting in the parabolic nature of the concentration profiles, as shown in Figure 4. The minimum was observed at the center of the membrane thickness. It may be noted that during desorption, the fraction of liquid molecules desorbed is equal to the fractional mass uptake if D is considered to be constant. Therefore, sorption and desorption curves shown in Figure 4 are symmetrical on either surface of the membrane. These curves showed a systematic variation with temperature (i.e., with an increase in temperature); the concentration profiles also increased, suggesting a relationship between the variation in concentration profiles and transport data (sorption, diffusion, or permeation).

The simulation method used in this study would serve as a sensitive test to predict the concentration profiles. It was further demonstrated that, with in-
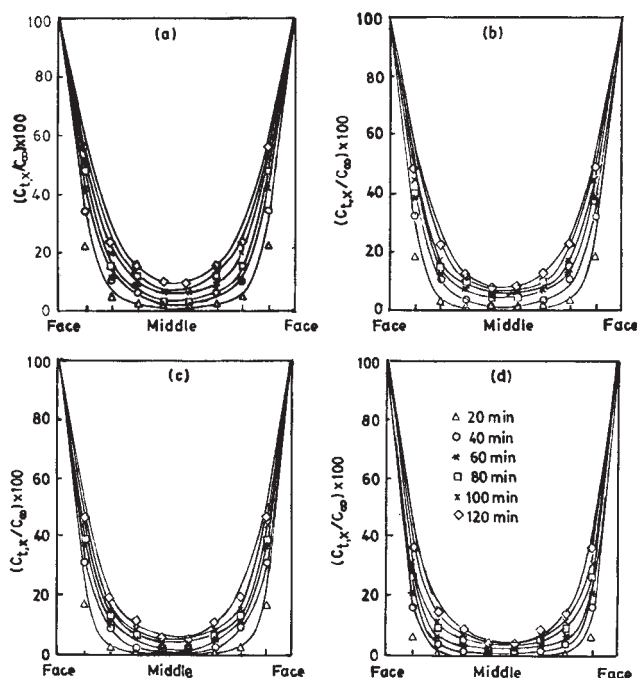
Figure 4 Concentration profiles calculated from eq. (10) for PU-1 with (a) *n*-hexane, (b) *n*-heptane, (c) *n*-octane, and (d) *n*-nonane at 25°C.

creasing immersion time, concentration profiles also increased dramatically. In the present study, it was found that these variations were quite substantial, further confirming that *D* values in these systems exhibited considerable concentration dependency, as seen by non-Fickian curvature trends of the sorption curves (see Figs. 1 and 2). This is especially significant in complicated systems such as the chain-extended PUs developed here. At any rate, the simulation method used here was useful in predicting the liquid concentration profiles, provided diffusion data of liquid–polymer systems are available.

CONCLUSIONS

In the present study, we have tried to identify factors that limit the long-term performance of chain-extended PUs by calculating sorption, diffusion, and permeation of *n*-alkanes (C_6–C_9) for the structurally different castor oil–based diol chain-extended PUs. Factors such as solvent type, chemical nature of PU, and their morphology have shown an influence on their transport characteristics. Lower diffusion coefficients observed for MDI- and TDI-based PUs than those of HMDI-based membranes were consistent with the morphological setup (physicomechanical properties) of PU membranes. Values of *n* were in the range of 0.554–0.612, suggesting that transport followed a Fickian mode. The ΔH^0 and ΔS^0 values for all PU–*n*-alkane systems were in the range of 41.57–91.45

kJ/mol and −38.82 to −26.39 J mol^{-1} K^{-1}, respectively. The negative values of ΔS^0 implied that solvent structures were retained even in the sorbed state. The positive values of ΔH^0 indicated an endothermic sorption process. Higher values of E_D and E_P were observed for distribution of hard segments in PUs rather than the soft segments, indicating the difficulty involved in molecular transport of liquids through the chosen membranes. From the simulation method used, it was demonstrated that by increasing the immersion time, concentration profiles also increased. The method could be used as a sensitive test to compute concentration profiles in any polymer–solvent system.

References

1. Varughese, K. T.; Nando, G. B.; De, P. P.; De, S. K. J Mater Sci 1988, 23, 3894.
2. Hepburn, C. Polyurethane Elastomers; Allied Science Publishers: London/New York, 1982.
3. Frisch, K. C.; Reegen, S. L. Advances in Urethane Science and Technology; Technomic: Westport, CT, 1976.
4. Kendaganna Swamy, B. K.; Siddaramaiah; Somashekar, R. J Mater Sci 2003, 38, 451.
5. Kendaganna Swamy, B. K.; Siddaramaiah. J Appl Polym Sci 2003, 90, 2945.
6. Aithal, U. S.; Aminabhavi, T. M.; Cassidy, P. E. J Membr Sci 1990, 50, 225.
7. Aithal, U. S.; Aminabhavi, T. M.; Shukla, S. S. J Chem Eng Data 1990, 35, 298.
8. Aithal, U. S.; Aminabhavi, T. M. Polymer 1990, 31, 1757.
9. Khinnavar, R. S.; Aminabhavi, T. M. J Appl Polym Sci 1991, 42, 2321.
10. Harogoppad, S. B.; Aminabhavi, T. M. J Appl Polym Sci 1991, 42, 2329.
11. Gibson, P. E. Properties in Polyurethane Block Copolymers—Development in Block Copolymers, I; Goodman, S., Ed.; Elsevier: London, 1982.
12. Trapps, G. Advances in Polyurethanes Technology; Buist, J. M.; Gudgeon, H., Eds.; Wiley–Interscience: New York, 1968.
13. Yen, M. S.; Chen, P.-Y.; Trai, H.-C. J Appl Polym Sci 2003, 90, 2824.
14. Aminabhavi, T. M.; Aithal, U. S. J Appl Polym Sci 1990, 41, 2112.
15. Khinnavar, R. S.; Aminabhavi, T. M. J Appl Polym Sci 1992, 46, 909.
16. Aminabhavi, T. M.; Phayde, H. T. S.; Ortego, J. D.; Vergnaud, J. M. Eur Polym J 1996, 32, 1117.
17. Vergnaud, J. M. Liquid Transport Processes in Polymeric Materials; Prentice Hall: Englewood Cliffs, NJ, 1991.
18. Aminabhavi, T. M.; Vijaya Kumar Naidu, B. J Appl Polym Sci 2004, 92, 991.

19. Aminabhavi, T. M.; Phayde, H. T. S.; Ortego, J. D.; Vergnaud, J. M. Polymer 1996, 37, 1677.

20. Harogoppad, S. B.; Aminabhavi, T. M. Macromolecules 1991, 24, 2598.

21. Crank, J. The Mathematics of Diffusion, 2nd ed.; Clarendon Press: Oxford, UK, 1975.

22. Zwolinski, B. J.; Eyring, H.; Reese, C. E. J Phys Colloid Chem 1949, 53, 1426.

23. Aithal, U. S.; Aminabhavi, T. M. J Chem Ed 1990, 67, 82.

24. Lucht, L. M.; Peppas, N. A. J Appl Polym Sci 1987, 33, 1557.

25. Chiou, J. S.; Paul, D. R. Polym Eng Sci 1986, 26, 1218.

26. Nicolais, L.; Drioli, E.; Hopfenberg, H. B.; Apicella, A. Polymer 1979, 20, 459.

27. Glasstone, S.; Laidler, K. J.; Eyring, H. Theory of Rate Processes; McGraw-Hill: New York, 1941.

28. Cassidy, P. E.; Aminabhavi, T. M.; Thompson, C. M. Rubber Chem Technol Rubber Rev 1983, 56, 594.

29. Wang, Y. Y.; Nakanishi, H.; Jean, Y. C. J Polym Sci Part B: Polym Phys 1990, 28, 1431.

30. Park, J. Y.; Paul, D. R. J Membr Sci 1997, 125, 23.

31. Bi, J. J.; Wang, C. L.; Kobayashi, Y.; Ogasawara, K.; Yamasaki, A. J Appl Polym Sci 2003, 87, 497.